Environmental Earth Sciences (2021) 80:520
https://doi.org/10.1007/s12665-021-09843-9

ORIGINAL ARTICLE

Saltwater intrusion in drinking water wells of Kordkuy, Iran: an integrated quantitative and graphical study

Esmaeil Ghezelsofloo[1] · Mostafa Raghimi[1] · Mojtaba G. Mahmoodlu[2] · Aziz Rahimi-Chakdel[1] · Seyed Mohammad Seyed Khademi[3]

Received: 29 December 2020 / Accepted: 28 July 2021 / Published online: 10 August 2021

Abstract

Seawater or saline water intrusion into coastal aquifers is one of the most challenging and widespread environmental problems that threaten the groundwater quality and sustainability. Extensive groundwater extraction in Kordkoy aquifer, mainly for municipality and agricultural development, has caused substantial seawater encroachment and upcoming of the deep saline water into the aquifer. This study was conducted to assess saline water intrusion into drinking water wells using hydrogeochemical approaches (quantitative and graphical). For this purpose, 28 water samples were collected from drinking water wells over two seasons to analyze 16 water quality parameters. The results of five chemical indicators encompass chloride concentration, Na/Cl, Ca/Mg, and Cl/($HCO_3 + CO_3$) ratios, and BEX indices revealed that more than 60% of drinking water wells in the study area were influenced by seawater or saline water. Furthermore, reverse ion exchange and salinization are the dominant ionic processes in the aquifer. The chemical indicator results, on the whole, were supported by various graphical techniques such as the bivariate plots of Cl versus EC, TDS versus Na/(Na + Cl), total dissolved ions (TDI) versus other major ions together with Stiff, Piper, Durov, HFD, and Gibbs diagrams. Results showed that except one well, which was harmfully contaminated by saline water, the sampling water wells, on the whole, were divided into three homogeneous chemical classes; unaffected, slightly, and moderately influenced by saline water. Since the preliminary results of geophysical surveys in the study area revealed a layer having an electrical resistivity of less than 5–10 Ωm in an average depth of 120 m, there is a quite high possibility of saline water intrusion from the subsurface layers due to high depth and discharge rate of some drinking wells.

Keywords Seawater intrusion · Coastal aquifer · Chemical indicators · Graphical approach

Introduction

Groundwater as a natural and precious resource plays a vital role in survival on the Earth and a key role in the existence of human society as well as in the growth and development of a country (Machiwal et al. 2018; Gopinath et al. 2019; Tiwari et al. 2019; Tran et al. 2020). Many coastal areas in the world contain dense populations, as these areas have food integrity and important economic activities such as urban development, trade, and touristic activities. These are factors that have attracted people to settle in these areas; consequently, the water demand for domestic consumption, agriculture, and industry has increased. For these above-mentioned reasons, a large quantity of water has long been pumped. As a result, ae common phenomenon, so-called seawater intrusion and/or groundwater salinization, has occurred in many coastal areas worldwide (Shi and Jiao

✉ Mojtaba G. Mahmoodlu
m.g.mahmnoodlu@gmail.com

Esmaeil Ghezelsofloo
ghezelsefloo@gmail.com

Mostafa Raghimi
m.raghimi@gu.ac.ir

Aziz Rahimi-Chakdel
a.rahimi@gu.ac.ir

Seyed Mohammad Seyed Khademi
seidkhademi@gmail.com

[1] Department of Geology, Golestan University, Gorgan, Iran

[2] Watershed and Rangeland Management, Gonbad Kavous University, Gonbad Kavus, Iran

[3] Department of Instrumental Analytical Chemistry, University of Duisburg-Essen, Duisburg, Germany

2014; Morgan and Werner 2015; Sae-Ju et al. 2018). However, anthropogenic activities contribute significantly to the deterioration of groundwater quality in coastal aquifers (Chidambaram et al. 2018).

In general, seawater intrusion is an environmental phenomenon in which the balance between salt water and fresh water is destroyed. The extent of seawater intrusion is mainly determined by three conditions: (1) the groundwater recharge rate, which depends on the infiltration capacity, stochastic characteristics of rainfall, climate factors climate, and geographic conditions, (2) the permeability of the coastal aquifers materials, and (3) the overextraction of groundwater (Shi and Jiao 2014; Ma et al. 2019).

Groundwater sources are the single-most important supply for the production of drinking water in the study area (Kordkuy City). The raw water from water abstraction wells is only disinfected with chlorine in a tank before entering the water distribution system of Kordkuy City. Recently, the amount of water production by drinking water wells and subsequently the extraction of groundwater have increased due to an increase in population growth. This reason, along with agriculture expansion and consequently the uncontrolled abstraction of groundwater by agricultural wells in the region, has increased the salinity in some drinking water wells supplying freshwater to Kordkuy City. This has become a main concern of the Water and Wastewater Company of Kordkuy City.

Investigation of saltwater intrusion is essential for sustainable groundwater resource management along the coastal regions. Mainly understanding of the aquifer hydrological system and the interaction between groundwater and seawater is important. It also helps to determine saline/seawater intrusion pathways (Tomaszkiewicz et al. 2014; Gopinath et al. 2019; Tiwari et al. 2019). Hence, over a period of 50 years, several international meetings have addressed the problem of marine intrusion (Saltwater Intrusion Meetings). Also, over the last century, a number of techniques have been extensively used to study saltwater intrusion including hydrogeochemistry and multivariate statistical approaches (Khadra and Stuyfzand 2016; Tran et al. 2020), geophysical methods (Kura et al. 2014; Paepen et al. 2018; Meyer et al. 2019), modeling and geographical information studies (Hu and Xu 2016; Gopinath et al. 2019).

Of the different techniques present for saltwater intrusion, the hydrogeochemistry method has been increasingly used to assess the saline water intrusion in the freshwater aquifers of many coastal regions across the globe. Over the past several decades, a number of hydrogeochemistry studies on saltwater intrusion has been carried out by many researchers in different coastal aquifers over the world (Mercado 1985; Xue et al. 2000; Tomaszkiewicz et al. 2014; Llopis-Albert et al. 2016; Kanagaraj et al. 2018; Chidambaram et al. 2018; Gopinath et al. 2019; Tran et al. 2020).

Current literature lacks information about the deterioration of groundwater quality and the possible saltwater intrusion in the study area. Therefore, the present study was performed to identify saltwater intrusion into drinking water wells drilled in the coastal aquifer of Kordkuy by applying various hydrogeochemical methods, together with geophysical profile tools over an area close to the coastal aquifer of Kordkuy City, Iran. The main objectives of the current study were to: (1) use several chemical indicators (e.g., chloride concentration, Na/Cl ratio, Simpson ratio, Ca/Mg ratio, Ca/(HCO_3 and SO_4, base exchange index), to distinguish sea water intrusion from other sources of salinity, (2) apply graphical approach (e.g., piper diagram, Durov diagram, hydrochemical facies evolution Diagram, and chloride concentration versus electrical conductivity) to identify saltwater intrusion into drinking water wells, and (3) determine and compare the statistical difference between the physicochemical parameters in the sampling wells in spring and fall.

Materials and methods

Study area

The study area, Kordkuy City, with a population of about 71,000 people and an area of around 545 ha is located in the SE of Caspian Sea and the west of Golestan Province (Fig. 1). Similar to numerous cities on the Caspian plain, Kordkuy City is situated on alluvial fan, so that the altitude decreases from south (419 m) to north (− 21 m below sea level).

From a geological point of view, the study area is located in Gorgan–Rasht and East Alborz zones and geological formations from old to new consist of Gorgan-green-schist (most of the heights of the region include these rocks and belong to the Ordovician), Lar Formation (consists of brownish limestone and dolomite with the age of upper Jurassic), alluvial sediments (mainly silt and sand, and peat with Quaternary age) and loess (predominantly silt-sized sediment with Quaternary age that is formed by the accumulation of wind-blown dust), respectively (Fig. 1).

Geophysical and hydrogeological study

Geoelectrical methods are applied to map the resistivity structure of the underground. Rock resistivity is of special interest for hydrogeological purposes: it allows, e.g., to discriminate between (1) freshwater and salt water, (2) soft-rock sandy aquifers and clayey material, (3) hard rock porous/fractured aquifers and low-permeable claystones and marlstones, and (4) water-bearing fractured rock and its solid host rock (Ernstson and Kirsch 2006).

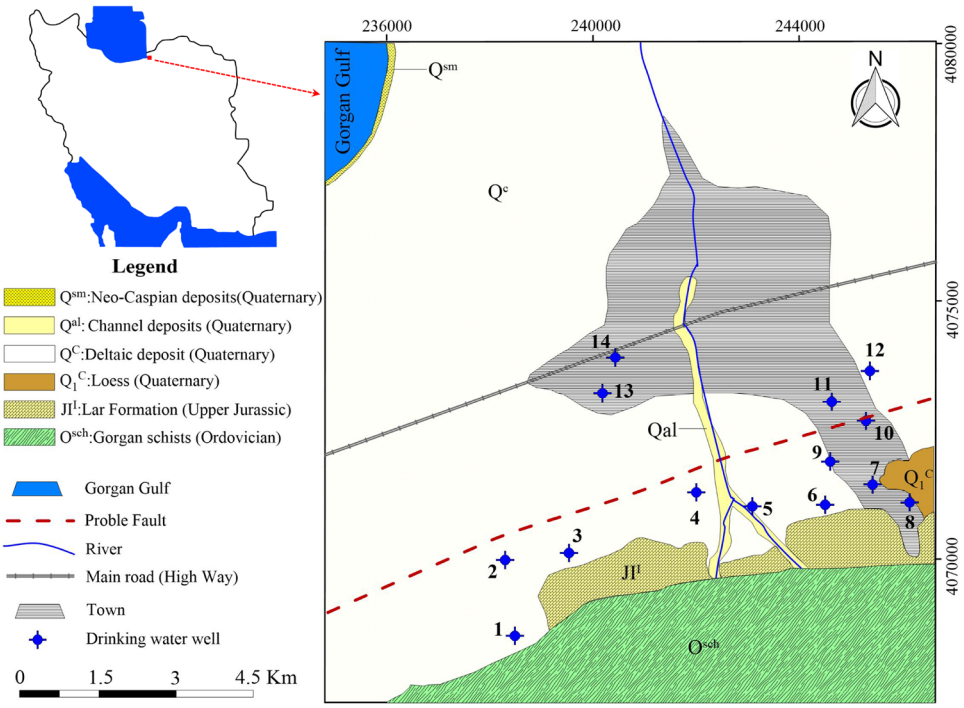

Fig.1 Geological map together with drinking (sampling) water wells

Figure 2 depicts a profile with north–south extensions from Kordkuy to Bandar Turkmen cities that has been studied by the General Geophysics Company. As shown in Fig. 2, three layers with different electrical resistivity were identified in the study area. The first layer has an electrical resistivity of about 20 Ωm, which changes to 15 Ωm to the north. This layer is the most superficial layer and is located just below the study area (Ghezelsofloo, 2019). The second layer is thicker and with an electrical resistivity of about 30 Ωm is located in the study area. However, its electrical resistivity increases to the south due to the aquifer recharge by the mountain front (50 Ωm). In contrast to the south, the electrical resistivity of the second layer diminishes to the north (less than 10 Ωm). The most probable reason for this can be the vicinity of mentioned layer to the Gorgan Gulf and subsequently saline water intrusion into it (Bouderbala and Remini 2014; Sae-Ju et al. 2018). The third layer starts from a depth of 100 m above the ground and apparently

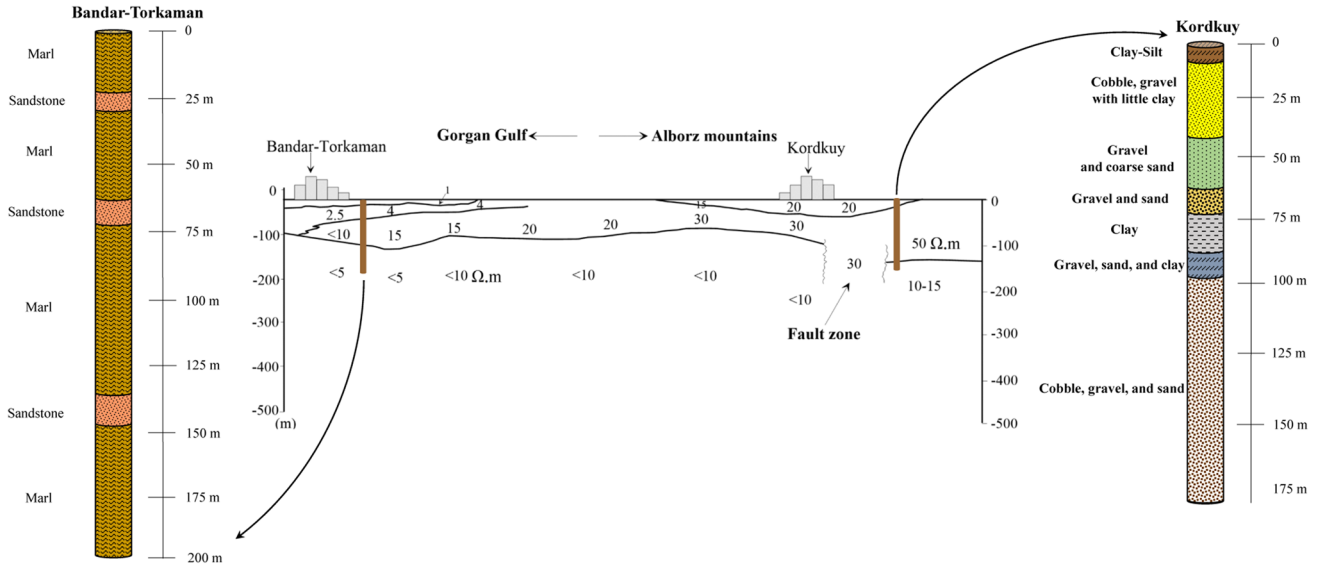

Fig. 2 Geoelectrical profile (**a**) together with the subsoil conditions of two existing boreholes along the geoelectric cross section in the study area

forms the bedrock of the aquifer. Throughout most areas, the third layer has an electrical resistivity of less than 10 Ωm, which decreases gradually to the north. One of the most important reasons for the reduction in the electrical resistivity of the third layer is the presence of water with high salinity (Bouderbala and Remini 2014; Sae-Ju et al. 2018). This saline water can also be due to the intrusion of seawater or the remnants of saline water (trap saline water) that has not been well washed by the freshwater front after Alpine Orogeny and the rise of Alborz Mountain. Most probably, saline water remains in deep layers due to the high density (Ghezelsofloo 2019).

An iso-depth map of the aquifer bedrock revealed that the shape of the Kordkuy aquifer resembles a bowl (Fig. 3a), the depression of which almost corresponds to the middle parts of the plain and decreases in thickness to the north and south. The maximum thickness of the aquifer is in the alluvial fan and the river route. Geophysical studies have not been able to determine the bedrock in this area. This may be because of the presence of sediments containing saline water (fossil or /and tapped water) under the freshwater aquifer. In fact, the boundary between the freshwater aquifer and sediments containing saline water was not a lithological unit.

The average groundwater level map in 2019 is depicted in Fig. 3b using monthly water level measurements of observation wells in the study area. The maximum groundwater level is situated in the floodplain of alluvial fan in the south of Kordkuy plain, and it gradually decreases toward the center of the plain. Based on the groundwater level map, the direction of groundwater flow to the north is along the topographic slope. Groundwater inlet sections are located in the south and on the edge of Alborz heights. Output sections are situated in the north of the study area. Results revealed that the highest hydraulic gradient is in the southern part of the plain and the lowest hydraulic gradient is in the northwest of the study area (Ghezelsofloo, 2019).

The maximum transmissivity in the northwest of the region is more than 1200 m^2/day and the minimum in the south of the region is about 800 m^2/day. Therefore, the amount of hydraulic conductivity (K) has a general trend in changes, so that the south of the plain (alluvial fan) due to the coarse-grained sand deposits has the highest amount, and to the north of the plain due to changes in grain size, the amount of K decreases. Also, the amount of storage coefficient in the plain varies from 1 to 8%.

Water sampling and analysis

In current research, 14 drinking water wells were selected to investigate the intrusion of saline water into the coastal aquifer (Fig. 1). The majority of drinking water wells in Kordkuy City have been drilled in in the southern part of this city on the floodplain of alluvial fan. The average depth of the drinking water is about 170 m. The drinking wells are 12 inches in diameter and have an average water production capacity of about 15 L/s per well. Drinking water supply wells in Kordkuy City mainly have different qualities.

The water samples were collected from the water sources using the sterile-polythene bottles of 600-ml capacity. Before sampling, bottles were washed with water of each sampling well to avoid any contamination. All water samples were collected in triplicate over spring and fall 2017. Then, the water samples were kept in a polyethylene bottle at 4 °C and transported to the Water and Wastewater Laboratory of Golestan Province for further laboratory analysis. Overall,

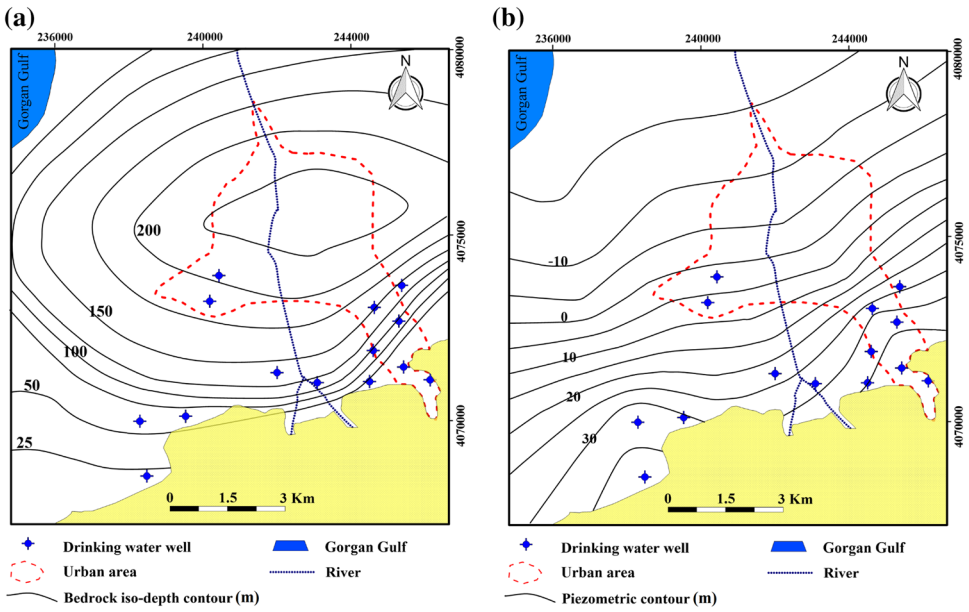

Fig. 3 Bedrock iso-depth map (**a**), and iso-piezometric map (**b**) of the study area

13 water physicochemical parameters were analyzed during the monitoring period (Table 1).

In this study, some parameters such as temperature (T), pH value, and electrical conductivity (EC) were determined in the field using a portable meter (WTW Multi 3430) and appropriate electrodes (WTW, Weilheim, Germany). The analytical procedures were developed following the American Public Health Association procedures (APHA 1995). The water samples were analyzed for bicarbonate (HCO_3^-) using acid titration method; chloride (Cl^-) using titration with silver nitrate ($AgNO_3$) as titrant; sulfate (SO_4^{2-}) measured by $BaCl_2$ method using spectrophotometer. Sodium (Na^+) and potassium (K^+) were analyzed using flame photometer. Calcium (Ca^{2+}) and magnesium (Mg^{2+}) were determined using the titration method. Nitrate (NO_3^-) concentration was estimated using a spectrophotometer (HACH, DR5000) following standard methods: cadmium redox and ascorbic acid with wavelength of 500 nm and 890 nm. The fluoride concentration of groundwater samples was determined using Metrohm 861 advanced compact ion chromatograph using appropriate standards (Brindha and Elango 2013).

Hydrogeochemistry

Quantitative approach

Over the last decades, several chemical indicators have been applied to distinguish seawater intrusion from other sources of salinity. These, as well as a few other indicators are described below.

The main cause of high chloride (Cl) in coastal aquifers is most likely attributed to seawater intrusion. Bear (1999) stated that an elevated chloride concentration can be used as an indication that seawater intrusion or pollution has occurred. The amount of Cl in groundwater can be used as a basis to classify its type, whether the groundwater is pure fresh water or water with high salt content (F = fresh:

Table 1 Physicochemical analysis of the selected drinking water well of Kordkuy in 2017

Season	Well	Depth	Q	pH	TH	TDS	EC	Ca^{2+}	Mg^{2+}	Na^+	K^+	HCO_3^-	SO_4^{2-}	Cl^-	NO_3^-	F^-
Spring	1	200	30	7.55	303	413	732	80.6	20.3	35.6	1.7	240	18.2	96.8	4.8	0.36
	2	144	90	7.53	240	364	671	65.5	16.5	42	1.2	260	15.7	56.9	3.12	0.35
	3	160	8.5	7.53	260	460	807	71.9	17.3	69	1.75	200	16.8	159.9	2.11	0.35
	4	132	8	7.79	380	375	744	85.2	19.2	40.7	0.99	244	18.5	96.4	3.3	0.48
	5	188	25	7.64	453	918	1776	145.8	34.8	172.2	2.6	236	18.4	452	3.8	1
	6	198	18	8.01	357	956	1743	187.5	59.8	74	1.8	236	17.2	460.6	2.7	0.6
	7	180	26	7.77	380	514	901	100.4	28.1	40.21	1.7	200	19.3	180.7	3.9	0.93
	8	200	12	7.86	271	480	816	91.1	27	35.4	1.5	240	18.1	132.8	3.3	0.78
	9	220	12	7.59	640	1453	2550	233.5	57	220.5	1.5	200	19.3	790	2.55	0.4
	10	151	25	7.63	389	1110	2140	139.3	42.9	195	2.2	240	17	531	8.2	1
	11	280	25	7.71	330	631	1107	95.8	20.4	112.6	2.1	236	18.6	235	13.5	0.6
	12	130	12	7.92	235	494	866	80.8	20.6	65.1	1.15	204	19.7	164.4	15.6	0.74
	13	200	6	7.95	230	254	468	55.3	12.8	13.2	0.67	220	15.3	15.19	3.8	0.3
	14	200	15	7.85	272	511	951	97.9	18.6	76.2	1.75	272	19.4	158.1	9.11	0.42
Autumn	1	200	30	7.76	310	495	868	95	26.3	42.4	1.8	300	17.2	116.1	4.56	0
	2	144	90	7.64	250	405	711	76.2	18	46	1.5	284	14.1	74.7	2.2	0.09
	3	160	8.5	7.8	270	531	931	86.4	14.6	86.6	1.5	276	14.4	156	1.42	0
	4	132	8	7.65	350	457	801	86	23	45	1.4	260	16.9	118.3	3	0.3
	5	188	25	7.56	510	1045	1840	164	40	152	2.4	300	15	454	2.35	0.1
	6	198	18	7.56	704	974	1709	183	56	75	1.65	268	16.4	433	2.73	0.24
	7	180	26	7.58	415	627	1092	120	32	49	1.8	272	17.9	207	2.95	0.07
	8	200	12	7.51	320	502	880	95	28	37	1.3	248	18.1	150.6	2.23	0
	9	220	12	7.41	700	1559	2735	236	65	235	5.3	220	17.8	822	2.5	0.38
	10	151	25	7.36	414	917	1582	120	34	150	5	292	18	363	12.7	0
	11	280	25	7.45	334	663	1160	100	24	102	2.3	260	17.6	238	11.2	0
	12	130	12	7.62	245	429	753	70	20	49	3.5	272	16.6	82	11.8	0
	13	200	6	7.84	250	317	556	71.1	17.2	14.5	1.2	276	14.8	28.5	3.6	0.01
	14	200	15	7.83	270	539	945	89.1	21.5	78	1.3	260	17.9	165	7.1	0.37

Here, anions, cations, TH, and TDS in mg/L, EC in µmho/cm, depth in meter, and Q in L/s)

Cl–\150 mg/L; Fb = fresh-brackish: 150–300 mg/L; B = brackish: 300–1000 mg/L; Bs = brackish-salt: 1000–10,000 mg/L and S = salt: 10,000–20,000 mg/L) (Klassen et al. 2014; Sudaryanto and Naily 2017).

Some research claimed that the ratio of Na/Cl can be utilized as an indication for seawater intrusion into coastal aquifers (e.g., Bear 1999; Klassen et al. 2014; Sudaryanto and Naily 2017). The ratios of Na/Cl are typically lower in wells intruded by seawater than in ocean water. As a result, the Na/Cl ratios less than 0.86 can represent the wells impacted by seawater intrusion. The Na/Cl ratios greater than one are typical of groundwater contaminated by anthropogenic sources.

The Simpson ratio (or Revelle Index) described by Todd (2001) is the ratio of $Cl/(HCO_3+CO_3)$ which is increasingly used to identify the degree of groundwater contamination by saline water (Simpson 1946). Based on the Simpson ratio, five classes were created to assess the level of contamination: first is good quality (< 0.5); second, slightly contaminated by saline water (0.5–1.3); third, moderately contaminated (1.3–2.8); fourth, injuriously contaminated (2.8–6.6), and highly contaminated (6.6–15.5) (Todd 2001; Klassen et al. 2014; Sudaryanto and Naily 2017).

An enrichment of Ca as the principal ion can also be used as an indicator of seawater intrusion into groundwater. High Ca/Mg and Ca/(HCO_3 and SO_4) ratios may indicate the onset of SWI (Bear et al. 1999), whereas if the ratio is greater than one (> 1), it means that seawater intrusion has been occurred.

Base exchange index (BEX) can also be used to discriminate whether an aquifer is undergoing salinization or freshening or has been freshened or salinized in the past. Among the different base exchange indices that have been compared and evaluated, Stuyfzand (2008) stated that the best index (for a dolomite free aquifer system) is BEX = Na + K + Mg − 1.0716 Cl (meq/L). A positive BEX represents freshening, a negative BEX indicates salinization and a BEX with a value of zero represents no base exchange (Stuyfzand 2008; Klassen et al. 2014; Sudaryanto and Naily 2017). For dolomitic aquifers BEXD = Na + K − 0.8768 Cl (meq/L) is proposed.

Graphical approach

Piper diagram has been widely used to classify hydrochemical facies on the basis of dominant ions (Piper 1944). It can be also used to identify the seawater intrusion, where chemical sample results are plotted based on the relative proportion major ions (Kelly 2006; Singaraja et al. 2012; Chidambaram et al. 2018). Generally, fresh groundwater samples will land near the area labeled as fresh water in the upper diamond, while pure seawater and or saline water will plot near the sea label (Kelly 2006). Water samples that result from conservative mixing (mixing without ionic exchange reactions) between fresh water and seawater would plot along the line labeled mixing. In general, once mixing occurs in the presence of aquifer materials, ion exchange reactions often occur between the groundwater and the aquifer material, which alters the chemical composition of the water. This change in chemical composition results in a deviation from the conservative mixing line on the piper diagram, moving the point upward into the upper portion of the diamond shape during intrusion, and downward toward the lower portion of the diamond during freshening. Using this method, it is possible to deduce not only if a water sample is impacted by saline water intrusion, but also if the intrusion was getting worse (intrusion exchange) or better (freshening exchange) at the time the sample was taken. In contrast, Durov diagram is a composite plot consisting of two ternary diagrams where the milliequivalents percentages of the cations of interest were plotted against that of anions of interest; sides form a central rectangular, binary plot of total cation vs. total anion concentrations (Ravikumar et al. 2015b).

A hydrochemical facies evolution diagram (HFE-diagram) is a multi-rectangular diagram, which is a useful tool in the interpretation of seawater intrusion processes (Fig. 4). This is a simple method for generating an HFE-D plot. An HFE-D considers the percentage of the four most significant ions and their relationships, giving 16 possible hydrochemical facies (32 if Mg^{2+} and SO_4^{2-} participate with HCO_3^- and Ca^{2+}). HFE-Diagram is described, which can assist in the interpretation of marine intrusion processes through the representation of the evolution of hydrochemical facies (Giménez-Forcada 2010; Giménez-Forcada 2019).

An elevated chloride concentration and electrical conductivity (EC) value are the simplest indicators of seawater intrusion or salinization. Principally, EC is positively correlated with the concentration of ions, mainly Cl concentration. Hence, a plot between Cl vs. electrical conductivity (EC) can be used as a common graphical method to distinguish seawater intrusion or salinization. In general, three zones on a plot of Cl vs. EC are distinguished: freshwater

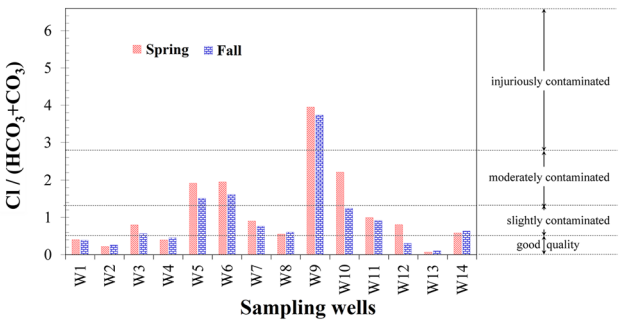

Fig. 4 Variation of the Simpson ratio values (Cl/HCO_3+CO_3) in the sampling wells

zone, mixing zone and intrusion zone. Groundwater samples with Cl exceeding 200 mg/L and EC exceeding ~ 1000 µS/cm are most likely influenced by seawater intrusion. Groundwater samples that are characterized by EC between 1000 and 5000 µS/cm represent a mixing between fresh water and salt water. Samples with EC of more than 10,000 µS/cm represent strong seawater influence (Lekshmi and Kani 2017; Alfarrah and Walraevens 2018).

Statistical analysis

In this study, *T* test was implemented to determine and compare the statistical difference between the physicochemical parameters in the sampling wells using Minitab statistical software. All data of physicochemical parameters were analyzed using completely randomized design. The assumptions of normality of data and equality of variances were first tested at the probability level of 5.0 percent. Then, *T* test and variance analysis were performed. The normality assumption of data was analyzed using the Anderson–Darling test. In this test, H_0 assumption having non-normality of data with a probability of 95% is accepted if the calculated P_{value} is greater than or equal to 5.0%. While the calculated P_{value} is less than 5.0%, H_0 assumption with a probability of 95% is rejected and H_1 assumption having non-normal data is accepted. The Levene tests were also used to determine the equality of variances at the probability level of 0.5%. Similar to Anderson–Darling test, if the calculated P_{value} is greater than or equal to 5.0%, then H_0 assumption (equality of variances) with a probability of 95% is accepted and H_1 assumption is rejected. When if the calculated P_{value} is less than 5.0%, H_0 assumption with a probability of 95% is rejected and H_1 assumption having equality of variances data is accepted.

Results and conclusions

Ionic process evaluation and ratio major ions

Statistical analysis of various chemical constituents in spring and fall seasons is given in Table 2. In this study, two assumptions of normality of data and similarity of variances were examined before performing the *T* test. Also, the significance level of 0.05 was considered. Results revealed that there was no statistical difference between two treatments, spring and fall, (except for pH, Fe, and SO_4).

In general, calcium and bicarbonate ions are dominant in fresh groundwater resources among the major anions and cations, respectively, in both seasons. Sodium and chloride ions are in second place. Furthermore, chloride ion in the sampling wells ranges from 15.19 to 822 mg/L representing great variations in the concentration of this ion in the study area.

Table 2 Results of *T* test for sampling well in spring and fall

Parameters	Test for equal variances	*p* value of *T* test
pH	0.550	0.046
TH	− 0.437	0.407
TDS	0.965	0.772
EC	0.854	0.929
Ca	0.905	0.817
Mg	0.975	0.760
Na	0.837	0.928
K	0.132	0.097
HCO3	0.801	0.669
SO4	0.773	0.019
Cl	0.883	0.916
NO3	0.982	0.669
F	0.041	0.000

Literature shows that a basic criterion for saline water intrusion assessment in the coastal aquifers can be the chloride content in groundwater (e.g., Klassen et al. 2014; Sudaryanto and Naily 2017; Ma et al. 2019). The sampling wells based on the chloride concentration are divided into three groups; (I) fresh (35.7%), (II) fresh–brackish (35.7%), and (III) brackish (28.6%). These results are consistent with the findings of earlier studies on the chloride concentration of groundwater in coastal aquifers that observed the high concentration of chloride in monitoring wells and stated the main cause of high chloride in coastal aquifers is most likely attributed to seawater intrusion (Klassen et al 2014; Alfarrah and Walraevens 2018; Ma et al. 2019).

Results of the Na/Cl ratio in all water samples were found to be less than 0.85 (Table 3). Low Na/Cl combined with other chemical indicator (e.g., an elevated chloride concentration.) also indicated that the aquifer had been intruded by seawater. Previous studies over several sites have reported similar results of the Na/Cl ratio representing a chemical indicators of saltwater intrusion (Klassen et al 2014; Nair et al. 2015; Lekshmi and Kani 2017). As given in Table 3, the Na/Cl ratio in well number 13 during spring was slightly larger than 0.85 (about 0.86). The location of well number 13 (drilled in urban area) and probably infiltration of urban wastewater into groundwater may cause an increase in Na concentration. However, the Na/Cl ratio became less than 0.85 (around 0.51) during fall.

The Simpson ratio (SR) was calculated and used to estimate the extent of contamination of Kordkuy drinking water wells from seawater intrusion (Table 3). SR obtained allow dividing the Kordkuy drinking water well samples in almost four homogeneous chemical groups. The first group (group I) with SR < 0.5 shows a good quality of sampling wells

Table 3 The ratio of major ions of groundwater to determine saltwater intrusion

Well	Na/Cl		Cl/HCO_3+CO_3		Ca/Mg		Na + K + Mg-1.071 Cl	
	Spring	Fall	Spring	Fall	Spring	Fall	Spring	Fall
1	0.37	0.37	0.40	0.39	3.97	3.61	0.34	0.55
2	0.74	0.62	0.22	0.26	3.97	4.23	1.49	1.26
3	0.43	0.56	0.80	0.57	4.16	5.92	− 0.36	0.29
4	0.42	0.38	0.40	0.46	4.44	3.74	0.46	0.31
5	0.38	0.33	1.92	1.51	4.19	4.10	− 3.23	− 3.75
6	0.16	0.17	1.95	1.62	3.14	3.27	− 5.71	− 5.16
7	0.22	0.24	0.90	0.76	3.57	3.75	− 1.35	− 1.44
8	0.27	0.25	0.55	0.61	3.37	3.39	− 0.21	− 0.60
9	0.28	0.29	3.95	3.74	4.10	3.63	− 9.52	− 9.11
10	0.37	0.41	2.21	1.24	3.25	3.53	− 4.97	− 1.52
11	0.48	0.43	1.00	0.92	4.70	4.17	− 0.47	− 0.72
12	0.40	0.60	0.81	0.30	3.92	3.50	− 0.41	1.39
13	0.87	0.51	0.07	0.10	4.32	4.13	1.18	1.21
14	0.48	0.47	0.58	0.63	5.26	4.14	0.11	0.21
Min	0.16	0.17	0.07	0.10	3.14	3.27	− 9.52	− 9.11
Max	0.87	0.62	3.95	3.74	5.26	5.92	1.49	1.39
Mean	0.43	0.40	1.24	1.06	4.05	4.02	− 1.92	− 1.55

and that there is no saline water intrusion occurred these wells (Fig. 4). In the study area, four wells (1, 2, 4, and 13) were unaffected by salt water. These are all (except W13) located in the margin of heights and close to groundwater inlet sections to the Kordkuy plain (Fig. 4). Despite the relatively high depth and also location (in urban area) of well number 13, the pumping rate of well is relatively low (6 L/s). This can be a reason for having a good water quality of the well. The second group ($0.5 < SR < 1.3$) contains six wells (42.86% of total wells) in the study area. The wells in group II were slightly influenced by saline water showing a mixture of fresh water and seawater. The wells in this group were distributed from the margin of heights to the north of study area. The third group with SR of 1.3 to 2.8 consists of three sampling wells (5, 6, and 10) representing.

Groundwater was moderately contaminated by saline water. Relatively high discharge rate of the wells in this group can be a possible reason for saltwater intrusion. The fourth group encompasses only one well which is injuriously contaminated by saline water. As shown in Fig. 4, well number 9 with SP of around 4.0 is the deepest well in the study area. This means that it is very close to bedrock of freshwater aquifer. Hence, there is quite a high possibility of saline water intrusion from the subsurface layers due to high depth of well. This can be a main reason for having high value of RI. Results for the Simpson ratio, on the whole, are consistent with the earlier studies (Klassen et al 2014; Hounsinou 2020; Putra et al. 2021).

As explained above, enrichment of Ca ($Ca/Mg > 1$) can indicate seawater intrusion (Bear et al. 1999). A total of 28 samples were used to calculate the Ca/Mg ratio and all of the wells had $Ca/Mg > 1$. This results are consistent with the findings of Klassen et al (2014).

The cation exchange is one of the most important reactions occurring in the coastal aquifers during saline water intrusion resulting in deficit of Na^+ and surplus of Ca^{2+} as follows (Alfarrah and Walraevens 2018; Shin et al. 2020):

$$2Na^+ + Ca - X_2 \rightarrow 2Na - X + Ca^{2+}, \quad (1)$$

where X represents the natural exchanger in the reaction. Hence, the base exchange indices (BEX) are frequently used to distinguish salinization and freshening of an aquifer (Alfarrah and Walraevens 2018; Shin et al. 2020). Hence, we estimated the BEX, as an indicator of cation exchange related to salinization or freshening of the aquifer (Table 3). Results revealed that more than 64% of wells indicate negative value of BEX. Thus it seems that the composition of drinking water wells is a result of ion exchange due to intrusion of saline water.

Graphical approach

In the current study, various graphical studies were used to identify saline water intrusion in Kordkuy aquifer. To evaluate the dominant ion process (ion exchange and reverse ion exchange) in the aquifer, the ratio of sodium to total sodium and chloride versus total dissolved solids (TDS) was used (Fig. 5). In this diagram, the ratio of sodium to total sodium and chloride is the main factor in determining the ion

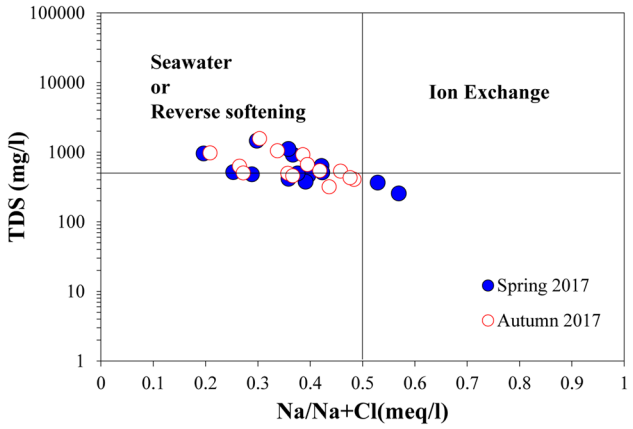

Fig. 5 Plot on the ratio of Na/Na + Cl versus TDS

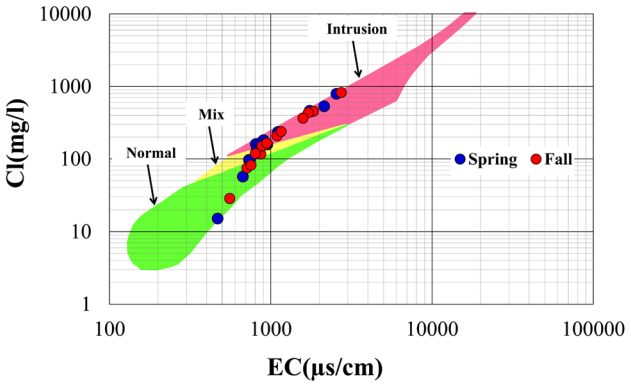

Fig. 6 A plot of chloride (Cl) vs. electrical conductivity (EC) showing normal groundwater conditions, saltwater intrusion, and mixing between the two

exchange process and vice versa ion exchange in the aquifer (Ravikumar et al. 2015a). A ratio of sodium ion to total sodium and chloride ions is less than 0.5 (Na/(Na + Cl)⟨0.5) indicates that the ion exchange process occurs in the aquifer, while a ratio of sodium ion to total sodium and chloride ions greater than 0.5 (Na/(Na + Cl)⟩0.5) indicates that reverse ion exchange is a dominant ionic process in the aquifer (Ravikumar et al. 2015a). Saline water intrusion into water resources is one of the most important factors that cause the reverse of the ion exchange process and ultimately salinization of water. Based on the distribution of samples for both seasons (spring and fall) in Fig. 5, the reverse ion exchange is a dominant process in the aquifer. Also, the distribution pattern of the samples shows the tendency of the groundwater to become saline and reach the chemical composition of seawater. This result is against that of Ravikumar et al. (2015a). They reported that ion exchange is a dominant process in a region of Bangalore North Taluk, Karnataka, India.

Figure 6 shows three zones (normal, mixed and SWI) on a plot of Cl vs. EC. It shows that groundwater samples with Cl exceeding 200 mg/L and EC exceeding ~ 1000 µs/cm are most likely influenced SWI. The majority of well samples that fall within the mix and seawater intrusion zones are considered to be influenced by seawater intrusion. Results for the plot of Cl vs. EC, on the whole, are consistent with earlier studies (Klassen et al 2014; Lekshmi and Kani 2017; Alfarrah and Walraevens 2018).

Generally, the bivariate plots are used to determine the geochemical processes of groundwater. In this research, we further used the bivariate plots to identify saline water intrusion. Figure 7 shows the plots of total dissolved ions (TDI) versus other major ions for the Kordkuy drinking water wells. Results revealed a linear distribution with a strong correlation between sodium and/or chloride with TDI. This resulted in mixing saline with fresh waters or dissolution of halite in water. As shown in Fig. 7, extrapolation intersects the x-axis in sodium and chloride ions plots. This is a sign of the importance of these two parameter compared to other ions. Furthermore, geoelctrical results (see above) indicated a layer having electrical resistivity of less than 10 Ω m. Therefore, mixing saline with fresh waters is the most probable reason for a linear distribution.

In addition to linear distribution, samples in all plots are grouped into three zones (A, B, and C) representing their chemical composition. The majority of wells are in zone A. Wells in this zone have two distinct characteristics: (1) calcium is the predominant cation and (2) TDI is less than 1000 mg/L. Zone B consists of three wells (W5, W6, and W10) that is similar to the third group in Stiff diagram and/or the Simpson ratio classifications. These wells show an increase in the concentration of chloride and sodium ions as well as TDS value. Zone C consists of only one well (W9) showing high concentration of sodium and chloride. Based on the chemical properties of wells located in zones B and C, the probability of saline water intrusion in wells 5, 6, 9, and 10 is higher than other wells in study area. These findings are, on the whole, consistent with the earlier study on the assessment of seawater intrusion using hydrochemical technique (Sae-Ju et al. 2018).

Stiff diagram patterns are very useful for a rapid visual comparison between water samples with different origin (Marqués et al. 2018). Similar to Simpson ratio, geometric shapes of Stiff diagrams obtained allow dividing the waters into four homogeneous chemical groups (Fig. 8). The first group consists of four wells with the dominant type of calcium bicarbonate, showing good quality of groundwater and not affected by saline water. This seems obvious considering the proximity of the study area to the heights (recharge area). The second group encompasses six wells with around 43% of total wells in the study area. The geometric shapes of Stiff diagrams together with their dominant water type (Ca–Cl) in this group show a mixture of fresh water and

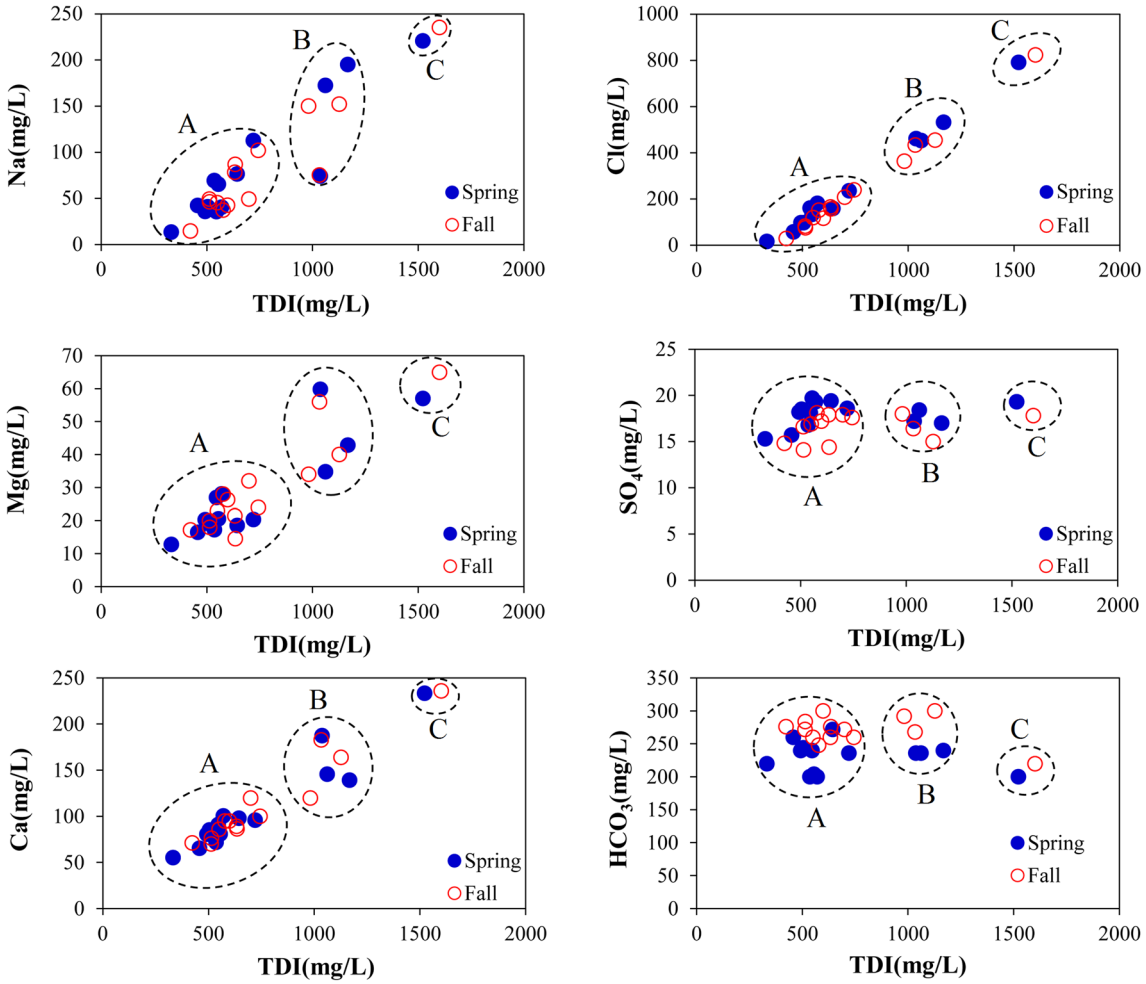

Fig. 7 Bivariate plots of major ions and total dissolved ions (TDI) in spring and autumn

seawater. As explained above, cation exchange is one of the most important reactions occurring in the coastal aquifers during saline water intrusion resulting in deficit of Na^+ and surplus of Ca^{2+}. Furthermore, the dominant Na^+ ions are adsorbed and Ca^{2+} ions released, so that the resulting water type moves from Na–Cl to Ca–Cl, which is typical for salinization (Alfarrah, and Walraevens 2018; Shin et al. 2020). The geometric shape of the Stiff diagrams in the third group is that of groundwater influenced by saline water. Similar to the SR results, the third group (including three wells 5, 6 and 10) clearly shows an increase in Cl ions and subsequently salinity and TDS of sampling wells (Fig. 8). Drilling depth, high rate of discharge, and function of Khazar fault are possible reasons for the increase in Cl concentration in these wells. Despite similarity of Stiff polygon in well number 9 with the third group, the value of TDS in this well is much greater than that of others wells. This can be a justifiable reason to consider the well number 9 as a separate group (fourth group).

In general, the term hydrochemical facies is used to describe the bodies of groundwater in an aquifer that differ in their chemical composition. The facies are a function of the lithology, solution kinetics, and flow patterns of the aquifer (Ravikumar and Somashekar 2011). To obtain the compositional trends and subsequent hydrochemical facies in groundwater and the mixing/migration path of the groundwater composition (evolutionary path) with the seawater/end solutions, Piper Diagram was further plotted using the major ions of sampling wells (Kelly 2006; Singaraja et al. 2012; Chidambaram et al. 2018). Preliminary results of Piper diagrams revealed that the dominant facies observed in the groundwater are of Ca–Mg–HCO_3 and Ca–Mg–Cl (Fig. 8a). Modified Piper diagram for saltwater intrusion purposed by Kelly (2006) revealed that majority of groundwater samples was in the zone of slight intrusion. Moreover, some groundwater samples (9 and 10) clearly show saltwater intrusion. Also, a few water samples are placed in the zone of freshening (Fig. 9a).

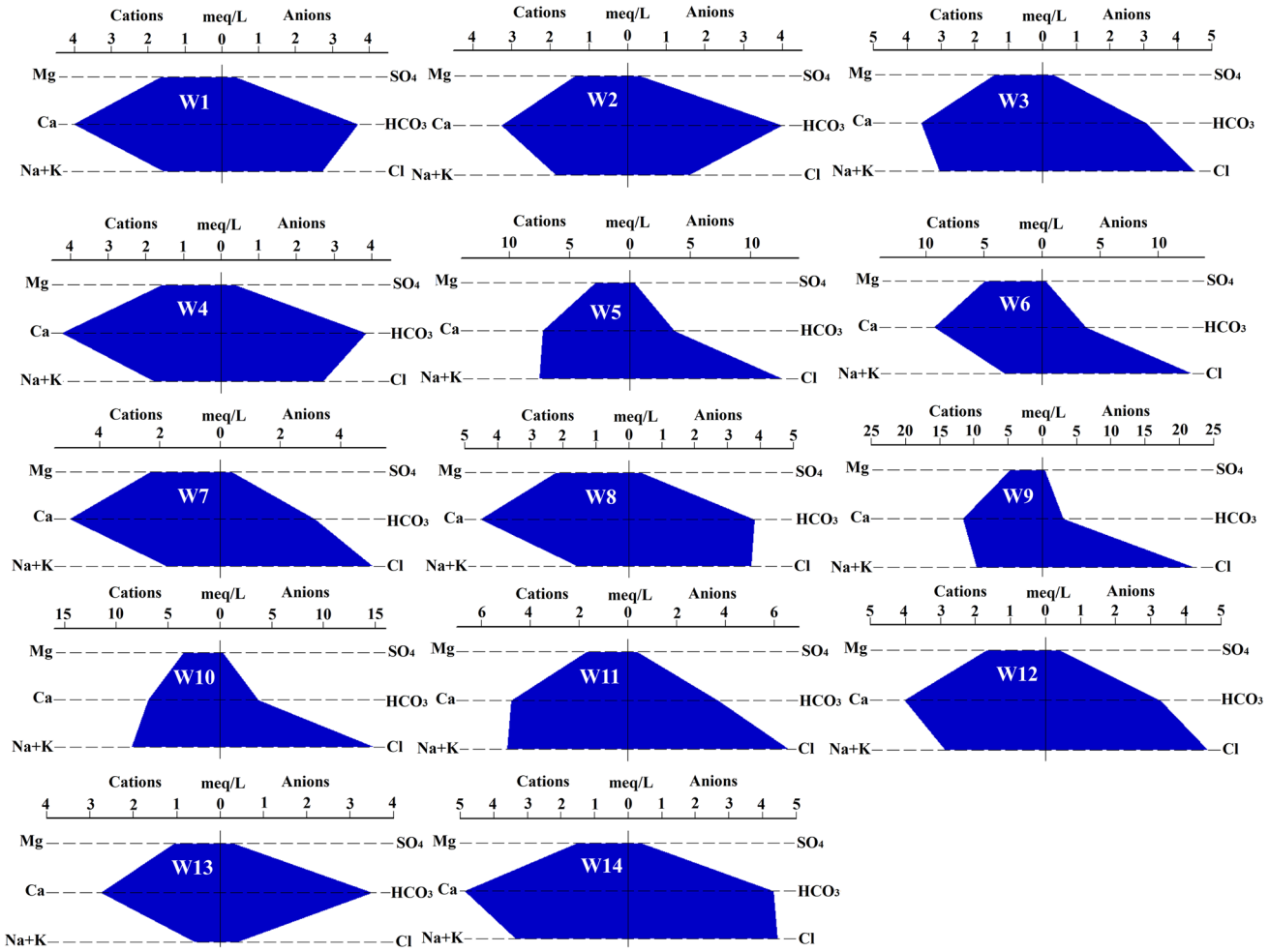

Fig. 8 Stiff diagrams of groundwater of sampling wells

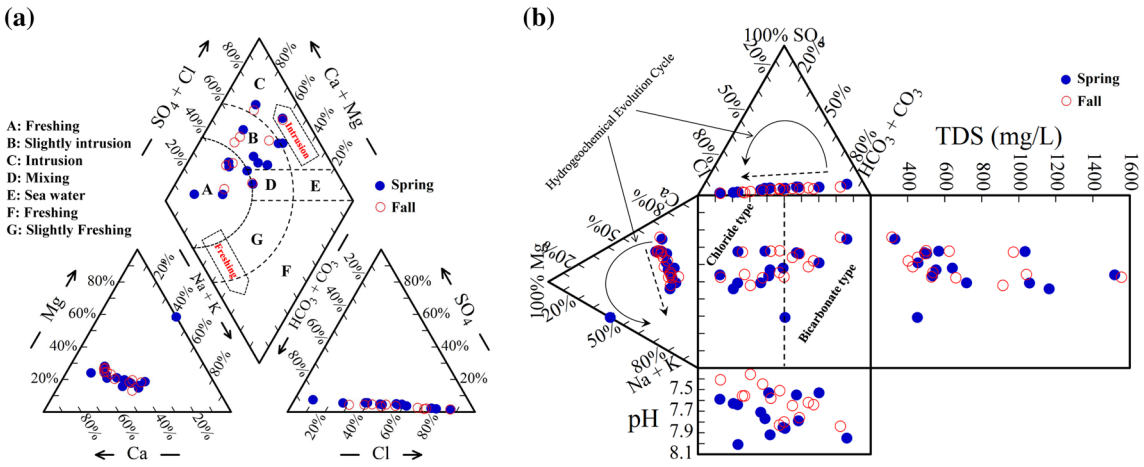

Fig. 9 Piper (**a**) and Durov (**b**) diagrams showing the hydrochemical types of groundwater and hydrochemical processes involved (Kelly 2006)

In this research, the Durov diagram was used for a better interpretation of the hydrogeochemistry facies and saltwater intrusion of Kordkuy aquifer (Fig. 9b). Based on the water samples distribution on Durov diagram, there is only one direction of geochemical evolution for Kordkuy groundwater. This ion evolution cycle is more consistent with the anion evolution cycle than the cation evolution cycle along the water flow path. The hydrogeochemical evolution of groundwater starts with the bicarbonate type in the recharge area (next to the highland margins) and ends with the chloride type in some wells. This trend can be clearly seen by increasing TDS of water samples in the rectangle part of Durov diagram. From the hydrogeochemical point of view, the described anion evolution sequence can be affected by two major variables: (1) the availability of the minerals and (2) the ability to dissolve the minerals. However, this evolution sequence can be altered by some factors such as the saltwater intrusion and/or the infiltration of urban and industrial wastewater into groundwater.

The HFE diagram as an alternative graphical diagram was applied to understand the hydrochemical facies as well as the spatiotemporal dynamics of the seawater intrusion process (Giménez-Forcada 2010; Giménez-Forcada 2019). As shown in Fig. 10, HFE-D diagram shows four facies including MixCa–Cl, Ca–$MixHCO_3$, Ca–HCO_3, and Ca–Cl for spring. The total facies increases to eight ($MixC–HCO_3$, $MixCa–MixHCO_3$, $Ca–MixHCO_3$, MixCa–MixCl, Ca–MixCl, MixCa–Cl, Ca–Cl, and MixNa–Cl) during fall season which shows more variety (Table 4). In the dry seasons, due to reduction in the aquifer recharge by the surface water and groundwater flow arising from the highlands, the water table and subsequently the pressure of the fresh water front become weaker (Fig. 10).

Table 4 Phase and facies of wells during spring and fall

Well	Phase		Facies	
	Spring	Fall	Spring	Fall
1	Intrus	Intrus	Ca–HCO_3	Ca–HCO_3
2	Fresh	Fresh	Ca–HCO_3	Ca–HCO_3
3	Intrus	Fresh	MixCa–Cl	MixCa–$MixHCO_3$
4	Intrus	Intrus	Ca–HCO_3	Ca–HCO_3
5	Intrus	Intrus	MixNa–Cl	MixCa–Cl
6	Intrus	Intrus	Ca–Cl	Ca–Cl
7	Intrus	Intrus	Ca–Cl	Ca–Cl
8	Intrus	Intrus	Ca–$MixHCO_3$	Ca–MixCl
9	Intrus	Intrus	MixCa–Cl	MixCa–Cl
10	Intrus	Fresh	MixNa–Cl	MixNa–Cl
11	Fresh	Intrus	MixNa–Cl	MixCa–Cl
12	Intrus	Fresh	MixCa–Cl	MixCa–HCO_3
13	Intrus	Intrus	Ca–HCO_3	Ca–HCO_3
14	Intrus	Intrus	Ca–$MixHCO_3$	MixCa–MixCl

Aquifer physical situation, mineralogy of bedrock, saline water intrusion, and weather condition can affect surface water and groundwater chemistry. The Gibbs diagram is a very important tool to determine geochemical processes (Marandi and Shand 2018). Hence, to illustrate the natural mechanism controlling groundwater chemistry consisting of the rainfall dominance, rock weathering dominance, and evaporation and precipitation dominance, Gibbs (1970) suggested two diagrams: (1) TDS versus $Na^+/(Na^+ + Ca^{2+})$ for cations and (2) TDS versus $Cl^-/(Cl^- + HCO_3^-)$ for anions. In modified version of Gibbs diagram for identifying saline water intrusion, evaporation and precipitation process are replaced by seawater (Fig. 11). Results of Gibbs diagram

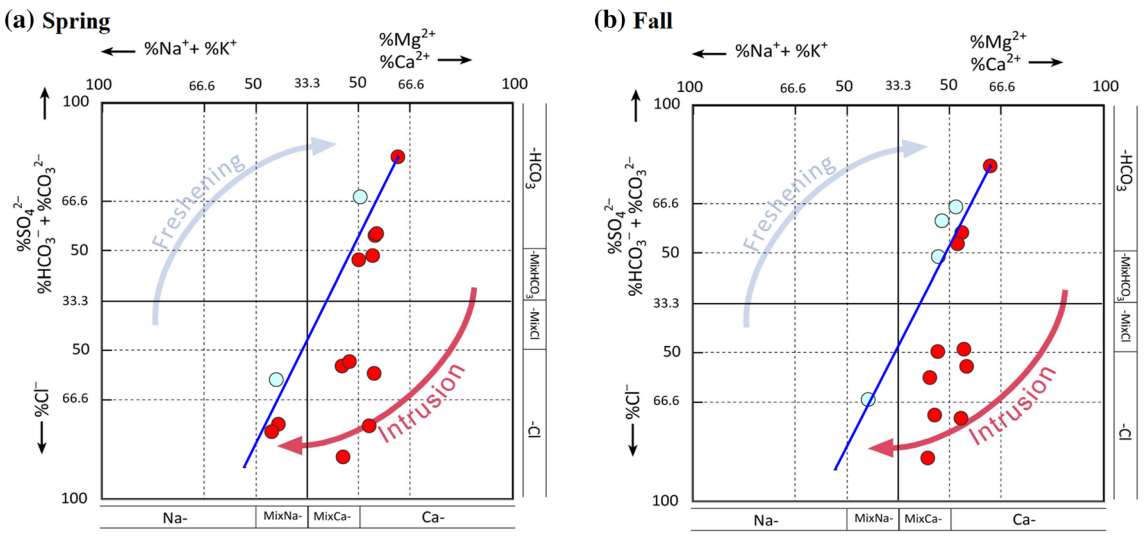

Fig. 10 HFE diagram to identify saltwater intrusion in drinking water wells of Kordkoy City

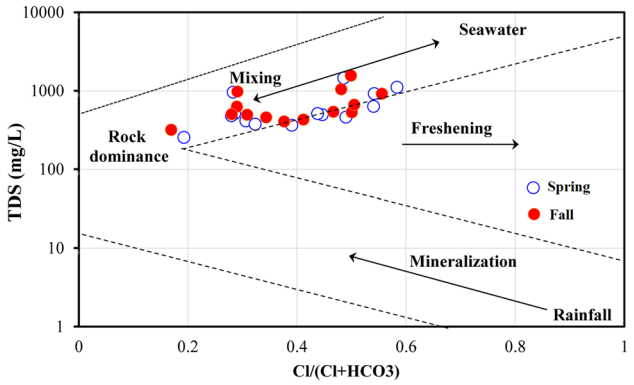

fig. 11 Gibbs diagram of drinking water wells in Kordkoy aquifer

revealed that the mixing of saline and fresh waters has occurred within a significant number of wells. Also, based on the distribution pattern of drinking water wells in Gibbs diagram, there is a tendency to change the chemical composition of groundwater and reach seawater composition.

Conclusion

Intensive groundwater abstraction from Kordkoy aquifer, mainly for municipality and agricultural development, has caused substantial seawater encroachment and upcoming of the deep saline water into the Kordkoy shallow aquifer. This study was conducted to assess saltwater intrusion in the fresh water aquifer using hydrogeochemical approach (quantitative and graphical approaches).

Statistical analysis results of various physicochemical parameters using the *T* test revealed that there was no statistical difference between the two treatments, spring and fall seasons, (except for pH, Fe, and SO_4). Results of the Na/Cl ratio together with Ca/Mg in all water samples indicated that all wells have been affected by seawater intrusion, as the ratios were greater than 0.86 and 1 for all of the sampling wells, respectively. Remarkable variation in the chloride concentration was observed in the study area. The sampling wells using the chloride concentration as a basic indicator were divided into three groups of fresh, fresh–brackish, and brackish. In contrast to the classification of water samples using chloride concentration, the sampling water wells were divided into four homogeneous chemical classes using the Simpson ratio (SR). The first class having SR < 0.5 shows a good quality of sampling wells and is subsequently unaffected by saline water. About 42.86% of the total wells were slightly influenced by saline water (0.5 < SR < 1.3) showing a mixture of fresh water and seawater. The third group having SR of 1.3 to 2.8 consists of three sampling wells representing that groundwater was moderately contaminated by saline water. The fourth group encompasses well number 9, which is harmfully contaminated by saline water. High drilling depth and discharge rate of the wells in the two last groups can be a possible reason for saltwater intrusion. Results of BEX as a useful indicator to distinguish salinization and freshening of an aquifer revealed that the composition of around 64% of water wells is a result of ion exchange due to intrusion of saline water.

Plot on the ratio of Na/Na + Cl versus TDS indicated that the reverse ion exchange is a dominant ionic process in the aquifer. Also, the distribution pattern shows the tendency of the groundwater to become saline and reach the chemical composition of seawater. The majority of well samples were in three zones of normal, mixed and seawater intrusion zones on the plot of Cl vs. EC. The plots of TDI versus other major ions for the Kordkuy drinking water wells revealed possible mixing of saline water with fresh waters or dissolution of halite in the aquifer. Also, the water samples in all plots are grouped into three zones (A, B, and C) representing their chemical composition similar to the plot of Cl vs. EC**.**

Similar to the results of the Simpson ratio, the geometric shapes of Stiff diagrams obtained allow dividing the waters into four homogeneous chemical groups. Except the first group which has good quality of groundwater, the other groups show different mixture of saline water with fresh groundwater (Ca–Cl to Na–Cl types). This is because of the cation exchange process occurring in the coastal aquifers during salinewater intrusion. The cation exchange process caused a deficit of Na^+ and surplus of Ca^{2+}. Furthermore, the dominant Na^+ ions are adsorbed by the natural exchanger (clay minerals) and Ca^{2+} ions released, so that the resulting water type moves from Na–Cl to Ca–Cl, which is typical for salinization.

Results of Piper and Durov diagram indicated that the majority of groundwater samples are landed in the zone of slightly intrusion. However, a few water samples are placed in the zone of fresh and intrusion zones. Groundwater facies in the study area alters from Ca–Mg–HCO_3 to Ca–Mg–Cl. Also, the hydrogeochemical evolution of groundwater starts with the bicarbonate type in the recharge area (next to the highland margins) and ends with the chloride type in some wells. In general, the described anion evolution sequence can be affected by two major variables: (1) the availability of the minerals and (2) the ability to dissolve the minerals. Moreover, the evolution sequence can be altered by some factors such as saltwater intrusion and/or the infiltration of urban and industrial wastewater into groundwater. Results of Na/Cl ratio showed that the saltwater intrusion is the most likely reason for altering the groundwater facies and subsequently the hydrogeochemical evolution. The HFE diagram as an alternative graphical diagram shows four facies including MixCa–Cl, Ca–MixHCO_3, Ca–HCO_3, and Ca–Cl for spring, while the total facies increases to eight (Mix Ca–HCO_3, Mix Ca–MixHCO_3, Ca–MixHCO_3,

MixCa–MixCl, Ca–MixCl, MixCa–Cl, Ca–Cl, and MixNa–Cl) during fall season which shows more variety. In the dry seasons, due to the reduction in the aquifer recharge by the surface water and groundwater flow arising from the highlands, the water table and subsequently the pressure of the fresh water front become weaker.

Gibbs diagram revealed that the mixing of saline and fresh waters had occurred in a significant number of wells. Also, based on the distribution pattern of drinking water wells in Gibbs diagram, there is a tendency to change the chemical composition of groundwater and reach seawater composition.

Since, preliminary results of geophysical investigations in the study area revealed a layer having electrical resistivity of less than 10 Ω m, there is a potential risk for the intrusion of deep saline water (beneath fresh aquifer) into fresh waters. Hence, to minimize or prevent saline water intrusion and subsequently deterioration of groundwater quality, viable solutions for the prevention of saline water intrusion into the freshwater aquifer can be reducing the discharge rate of the drinking water wells, drilling new wells in the floodplain of alluvial fan in the study area and skimming well with a horizontal collector system.

References

Alfarrah N, Walraevens K (2018) Groundwater overexploitation and sea water intrusion in coastal areas of arid and semi-arid regions. Water 10(2):143

Bear J (1999) Seawater intrusion in coastal aquifers: concepts, methods and practices. Mass: Kluwer Academic, Boston

Bouderbala A, Remini B (2014) Geophysical approach for assessment of seawater intrusion in the coastal aquifer of Wadi Nador (Tipaza, Algeria). Acta Geophys 62(6):1352–1372

Brindha K, Elango L (2013) Geochemistry of fluoride rich groundwater in a weathered granitic rock region, Southern India. Water Qual Expo Health 5(3):127–138

Chidambaram S, Sarathidasan J, Srinivasamoorthy K, Thivya C, Thilagavathi R, Prasanna MV, Singaraja C, Nepolian M (2018) Assessment of hydrogeochemical status of groundwater in a coastal region of Southeast coast of India. Appl Water Sci 8(1):27

Ernstson K, Kirsch R (2006) Geoelectrical methods. Groundw Geophys Tool Hydrogeol 1:84–117

Ghezelsofloo E (2019) The use of hydrogeochemical methods to determine saltwater intrusion into Kordkuy Coastal Aquifer, Golestan Province. MSc thesis in Golestan University (in Persian only)

Gibbs RJ (1970) Mechanisms controlling world water chemistry. Science 170(3962):1088–1090

Giménez-Forcada E (2010) Dynamic of sea water interface using hydrochemical facies evolution diagram. Groundwater 48(2):212–216

Giménez-Forcada E (2019) Use of the Hydrochemical Facies Diagram (HFE-D) for the evaluation of salinization by seawater intrusion in the coastal Oropesa Plain: comparative analysis with the coastal Vinaroz Plain, Spain. HydroResearch 2:76–84

Gopinath S, Srinivasamoorthy K, Saravanan K, Prakash R, Karunanidhi D (2019) Characterizing groundwater quality and seawater intrusion in coastal aquifers of Nagapattinam and Karaikal, South India using hydrogeochemistry and modeling techniques. Human Ecol Risk Assess Int J 25(1–2):314–334. https://doi.org/10.1080/10807039.2019.1578947

Hounsinou SP (2020) Assessment of potential seawater intrusion in a coastal aquifer system at Abomey-Calavi Benin. Heliyon 6(2):e03173. https://doi.org/10.1016/j.heliyon.2020.e03173

Hu BX, Xu, Z (2016) Data analysis and numerical modeling of seawater intrusion through conduit networks in a coastal karst aquifer, 24th Salt Water Intrusion Meeting and the 4th Asia-Pacific Coastal Aquifer Management Meeting, 4–8 July 2016, Cairns, Australia

Kanagaraj G, Elango L, Sridhar SGD, Gowrisankar G (2018) Hydrogeochemical processes and influence of sea water intrusion in coastal aquifers south of Chennai, Tamil Nadu India. Environ Sci Pollut Res 25(9):8989–9011. https://doi.org/10.1007/s11356-017-0910-5

Kelly DJ (2006) Development of seawater intrusion protection regulations. In: Proceedings 1st SWIM-SWICA Joint Saltwater Intrusion Conference. Cagliari-Chia Laguna, Italy 135–145

Khadra WM, Stuyfzand PJ (2016) Mass balancing to define major hydrogeochemical processes in salinizing dolomitic limestone aquifers: Example from Eastern Mediterranean (Lebanon), 24th Salt Water Intrusion Meeting and the 4th Asia-Pacific Coastal Aquifer Management Meeting, 4–8 July 2016, Cairns, Australia

Klassen J, Aleen DM, Kirtse D (2014) Chemical indicators of saltwater intrusion for the Gulf Islands. Final Report, Department of Earth Sciences, Simon Rfaser University, British Columbia

Kura NU, Ramli MF, Ibrahim S, Sulaiman WNA, Zaudi MA, Aris AZ (2014) A preliminary appraisal of the effect of pumping on seawater intrusion and upconing in a small tropical island using 2D resistivity technique. Sci World J 796425:11. https://doi.org/10.1155/2014/796425

Lekshmi S, Kani KM (2017) Assessment of seawater intrusion using chemical indicators. International Journal of Engineering and Advanced Technology (IJEAT), December 13–15, 2017. TKM College of Engineering, Kollam (Kerala), India 7:100–1007

Llopis-Albert C, Merigó JM, Xu Y (2016) A coupled stochastic inverse/sharp interface seawater intrusion approach for coastal aquifers under groundwater parameter uncertainty. J Hydrol 540:774–783

Ma J, Zhou Z, Guo Q, Zhu S, Dai Y, Shen Q (2019) Spatial characterization of seawater intrusion in a coastal aquifer of northeast Liaodong Bay China. Sustainability 11(24):7013

Machiwal D, Cloutier V, Güler C, Kazakis N (2018) A review of GIS-integrated statistical techniques for groundwater quality evaluation and protection. Environ Earth Sci 77(19):681

Marandi A, Shand P (2018) Groundwater chemistry and the Gibbs diagram. J Appl Geochem 97:209–212. https://doi.org/10.1016/j.apgeochem.2018.07.009

Marqués AL, Ribeiro L, Roqueñí N, Fernández JJ, Loredo J (2018) A new graphic methodology to interpret the multivariate data analysis of hydrochemical data in orphan mine areas. J Geochem Explor 191:43–53. https://doi.org/10.1016/j.gexplo.2018.06.001

Mercado A (1985) The use of hydrogeochemical patterns in carbonate sand and sandstone aquifers to identify intrusion and flushing of saline water. Groundwater 23(5):635–645

Meyer R, Engesgaard P, Sonnenborg TO (2019) Origin and dynamics of saltwater intrusion in a regional aquifer: combining 3-D salt water modeling with geophysical and Geochemical Data. Water Resour Res 55(3):1792–1813. https://doi.org/10.1029/2018WR023624

Morgan LK, Werner AD (2015) A national inventory of seawater intrusion vulnerability for Australia. J Hydrol Reg Stud 4:686–698. https://doi.org/10.1016/j.ejrh.2015.10.005

Nair IS, Rajaveni SP, Schneider M, Elango L (2015) Geochemical and isotopic signatures for the identification of seawater intrusion in an alluvial aquifer. J Earth Syst Sci 124(6):1281–1291

Paepen M, Michael H, Walraevens K, Hermans T(2018) Assessment of groundwater discharge and saltwater intrusion in the Belgian coastal area through geophysics, 25th Salt Water Intrusion Meeting, 17-22 June 2018, Gdansk, Poland

Piper AM (1944) A graphic procedure in the geochemical interpretation of water-analyses. Eos Trans Amer Geophys Union 25(6):914–928

Putra DBE, Hadian MSD, Alam BYCS, Yuskar Y, Yaacob WZW, Datta B, Harnum WPD (2021) Geochemistry of groundwater and saltwater intrusion in a coastal region of an island in Malacca Strait. Indonesia Environ Eng Res 26(2):1–8. https://doi.org/10.4491/eer.2020.006

Ravikumar P, Somashekar RK (2011) A geochemical assessment of coastal groundwater quality in the Varahi river basin Udupi District, Karnataka State, India. Arab J Geosci 6:1855–1870. https://doi.org/10.1007/s12517-011-0470-9

Ravikumar P, Mohammad Aneesul M, Somashekar RK (2015a) Interpretation of groundwater quality and radon estimation in the selected region of Bangalore North Taluk, Karnataka, India. Res Rev J Ecol Environ Sci 3(2):73–81

Ravikumar P, Somashekar RK, Prakash KL (2015b) A comparative study on usage of Durov and Piper diagrams to interpret hydrochemical processes in groundwater from SRLIS river basin, Karnataka, India. Elixir Int J 80:31073–31077

Sae-Ju J, Chotpantarat S, Thitimakorn T (2018) Assessment of seawater intrusion using multivariate statistical, hydrochemical and geophysical techniques in coastal aquifer, Cha-am district, Thailand. Hydrol Earth Syst Sci Discuss. https://doi.org/10.5194/hess-2018-137

Shi L, Jiao JJ (2014) Seawater intrusion and coastal aquifer management in China: a review. Environ Earth Sci 72:2811–2819. https://doi.org/10.1007/s12665-014-3186-9

Shin K, Koh DC, Jung H, Lee J (2020) The hydrogeochemical characteristics of groundwater subjected to seawater intrusion in the Archipelago. Korea Water 12(6):1542. https://doi.org/10.3390/w12061542

Simpson TR (1946) Salinas basin investigation bull Calif. Div Water Resour Sacram 52:230

Singaraja C, Chidambaram S, Anandhan P, Prasann MV, Thivya C, Thilagavathi R (2012) A study on the status of fluoride ion in groundwater of coastal hard rock aquifers of south India. Arab J Geosci 6(11):4167–4177. https://doi.org/10.1007/s12517-012-0675-6

Stuyfzand PJ (2008) Base exchange indices as indicators of salinization or freshening of (coastal) aquifers. In: Proceedings of 20th Salt Water Intrusion Meeting. Florida, June 23–27, 2008: 262–265

Sudaryanto M, Naily W (2017) Ratio of major ions in groundwater to determine saltwater intrusion in coastal areas. Global Colloq GeoSci Eng. https://doi.org/10.1088/1755-1315/118/1/012021

Tiwari AK, Pisciotta A, De Maio M (2019) Evaluation of groundwater salinization and pollution level on Favignana Island, Italy. Environ Pollut 249:969–981. https://doi.org/10.1016/j.envpol.2019.03.016

Todd DK (2001) Groundwater hydrology. Wiley, USA (**SBN: 978-0-471-05937-0**)

Tomaszkiewicz M, Abou Najm M, El-Fadel M (2014) Development of a groundwater quality index for seawater intrusion in coastal aquifers. Environ Model Softw 57:13–26. https://doi.org/10.1016/j.envsoft.2014.03.010

Tran DA, Tsujimura M, Kambuku D, Dang TD (2020) Hydrogeochemical characteristics of a multi-layered coastal aquifer system in the Mekong Delta Vietnam. Environ Geochem Health 42(2):661–680. https://doi.org/10.1007/s10653-019-00400-9

Xue Y, Wu J, Ye S, Zhang Y (2000) Hydrogeological and hydrogeochemical studies for salt water intrusion on the south coast of Laizhou Bay China. Groundwater 38(1):38–45. https://doi.org/10.1111/j.1745-6584.2000.tb00200.x